JACS
JOURNAL OF THE AMERICAN CHEMICAL SOCIETY
Article
pubs.acs.org/JACS

Following Metabolism in Living Microorganisms by Hyperpolarized ^{1}H NMR

Piotr Dzien,[†,‡,§] Anne Fages,[∥,§] Ghil Jona,[⊥] Kevin M. Brindle,[‡] Markus Schwaiger,[†] and Lucio Frydman*[,∥]

[∥]Department of Chemical Physics and [⊥]Biological Services Unit, Weizmann Institute, Rehovot 76100, Israel
[†]Klinik und Poliklinik für Nuklearmedizin, Technische Universität München, München 81675, Germany
[‡]Cancer Research UK Cancer Institute, Cambridge CB2 0RE, United Kingdom

Supporting Information

ABSTRACT: Dissolution dynamic nuclear polarization (dDNP) is used to enhance the sensitivity of nuclear magnetic resonance (NMR), enabling monitoring of metabolism and specific enzymatic reactions in vivo. dDNP involves rapid sample dissolution and transfer to a spectrometer/scanner for subsequent signal detection. So far, most biologically oriented dDNP studies have relied on hyperpolarizing long-lived nuclear spin species such as ^{13}C in small molecules. While advantages could also arise from observing hyperpolarized ^{1}H, short relaxation times limit the utility of prepolarizing this sensitive but fast relaxing nucleus. Recently, it has been reported that ^{1}H NMR peaks in solution-phase experiments could be hyperpolarized by spontaneous magnetization transfers from bound ^{13}C nuclei following dDNP. This work demonstrates the potential of this sensitivity-enhancing approach to probe the enzymatic process that could not be suitably resolved by ^{13}C dDNP MR. Here we measured, in microorganisms, the action of pyruvate decarboxylase (PDC) and pyruvate formate lyase (PFL)—enzymes that catalyze the decarboxylation of pyruvate to form acetaldehyde and formate, respectively. While ^{13}C NMR did not possess the resolution to distinguish the starting pyruvate precursor from the carbonyl resonances in the resulting products, these processes could be monitored by ^{1}H NMR at 500 MHz. These observations were possible in both yeast and bacteria in minute-long kinetic measurements where the hyperpolarized ^{13}C enhanced, via ^{13}C → ^{1}H cross-relaxation, the signals of protons binding to the ^{13}C over the course of enzymatic reactions. In addition to these spontaneous heteronuclear enhancement experiments, single-shot acquisitions based on *J*-driven ^{13}C → ^{1}H polarization transfers were also carried out. These resulted in higher signal enhancements of the ^{1}H resonances but were not suitable for multishot kinetic studies. The potential of these ^{1}H-based approaches for measurements in vivo is briefly discussed.

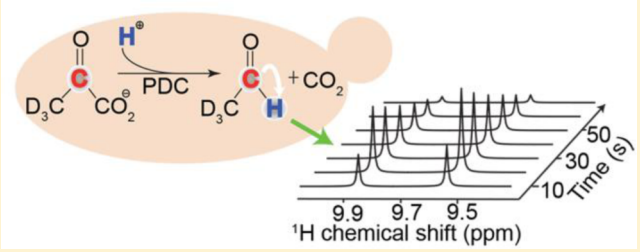

1. INTRODUCTION

Magnetic resonance (MR) in either its spectroscopic (NMR) or its imaging (MRI) modalities is a leading method for characterizing the nature, dynamics, and location of biochemical processes. Despite this versatility, the very low energies involved in MR mean that only a very small fraction of the pool of potentially active nuclei—on the order of 10–100 ppm—gives rise to observable signals. This creates particular challenges for in vivo MR spectroscopy, which focuses on measurements of metabolites that are present in the micromolar to millimolar range. Recent research has demonstrated that by increasing the nuclear spin polarization from thermal equilibrium to metastable hyperpolarized states the sensitivity of NMR and MRI can be increased ca. 10 000–100 000 fold.[1] Such nuclear hyperpolarization methods are based on the use of electron → nuclear magnetization transfer by dynamic nuclear polarization (DNP),[1a] on transferring spin order to nuclei from para-hydrogen singlet states,[2,3] or on coupling photon polarization with nuclear spin alignment by optical pumping.[4] Dissolution dynamic nuclear polarization (dDNP), in particular, has emerged in the past decade as arguably the most general of all these biomolecular methods. dDNP utilizes the rapid and efficient electron spin polarization in a high magnetic field at low (~1 K) temperatures and transfers this polarization, via microwave irradiation, to adjacent nuclear spins. Once the targeted nuclear spins are hyperpolarized in the solid state, the sample is rapidly brought to room temperature by dissolving it with a pressurized, superheated solvent. The hyperpolarized (HP) sample is then transferred to a MR scanner for liquid-state measurements and can, in principle, provide signal-to-noise ratio (SNR) enhancements on the order of the increase imparted onto the nuclear spin polarization, i.e., 10 000–100 000×. To make such unprecedented gains compatible with in cell and in vivo observations, the HP spins have to withstand the polarization losses associated with their transfer from the cryogenic state where they are generated to the NMR magnet where they are

Received: July 20, 2016
Published: August 24, 2016

DOI: 10.1021/jacs.6b07483
J. Am. Chem. Soc. 2016, 138, 12278–12286

observed. One of dDNP's weaknesses lies in the T_1 relaxation that nuclear spins undergo during this transit between the polarizing and the observation magnets, which is compounded by the paramagnetic relaxation effects of the free-radical polarizing agent. Adding to these losses, particularly in vivo, will be the additional delay resulting from the time taken for the polarized substrate to reach the tissue of interest and for its subsequent metabolism. Consequently, most in vivo dDNP studies focus on hyperpolarizing nuclei with low gyromagnetic ratios γ possessing relatively long T_1 relaxation times, such as nonprotonated ^{13}C or ^{15}N in small molecules. Clearly, however, advantages could also result from observations based on hyperpolarizing and observing high-γ nuclei, such as ^{1}H. Since for a given field and polarization level the signal detected by NMR's inductive method is proportional to $|\gamma|^2$, the γ^{1H}/γ^{13C} ratio of 4 predicts a roughly 16-fold gain in signal intensity.[5] While this gain will be moderated by a concomitant increase in spectral noise with frequency, the fact that ^{1}H-observation hardware is the most widely available and, arguably, the most mature of all in vivo MR technologies, could further enhance these observations. Lastly, instances may arise where ^{1}H-based observations provide a better chemical discrimination than ^{13}C-based ones.

Despite these considerations, ^{1}H-based hyperpolarized MR observations are challenged by short relaxation times T_1^H leading to the depolarization. Still, it has been shown that polarized water can be used to enhance the sensitivity of NMR on unfolded peptides,[6] and also for ^{1}H MR angiography.[7] Another possible solution to the problem of a short T_1^H rests in "storing" the hyperpolarization in a nuclear spin state with a slow relaxation time, for instance, in long-lived singlet spin states, shown to be accessible in certain systems involving two coupled spin-1/2 nuclei.[8] Yet another ^{1}H-enabling approach relies on imparting hyperpolarization on a slowly relaxing, low-γ nucleus, and then enhancing the ^{1}H MR signal by transferring polarization to the latter from the low-γ species using a suitable pulse sequence such as INEPT.[9] Unless special precautions are taken, however,[9d,10] this will deplete the hyperpolarization of the low-γ nucleus in a single acquisition, thereby limiting the usefulness of this approach for following kinetics.

Recently, spontaneous enhancements in solution-phase ^{1}H NMR of hydrogens covalently bound to HP ^{13}C spins have been reported.[11] Heteronuclear cross-relaxation effects arising in rapidly tumbling small molecules were identified as the mechanism responsible for this ^{13}C → ^{1}H polarization transfer. The fact that in these experiments hyperpolarization can be stored in a relatively slowly relaxing ^{13}C nucleus that will then share, over a tens-of-seconds time scale given by T_1^C, its hyperpolarization with a neighboring ^{1}H, opens the possibility of using the latter signals to monitor enzymatic turnover. This could, in turn, facilitate monitoring metabolic processes with the sensitivity of ^{1}H NMR using the more widespread, single-channel hardware available in ^{1}H MRI for in vivo detection. This approach may also improve spectral resolution, particularly in cases where the enzymatic transformations involve the addition of a hydrogen atom. Two such processes are demonstrated in the present work, both in vitro using solutions of purified enzymes, as well as in suspensions of intact cells. The starting substrate in these two studies was HP [^{13}C]-pyruvate, a metabolite whose cell biochemistry lies at the interface between catabolic and anabolic metabolism. The enzymatic processes targeted were (i) the production of acetaldehyde following the addition of HP [U-^{2}H$_3$,2-^{13}C]-pyruvate to samples containing purified pyruvate decarboxylase (PDC) from *S. cerevisiae* and to *S. cerevisiae* cultures fermenting glucose, and (ii) the generation of formic acid due to the activity of pyruvate formate lyase (PFL), measured in cultures of anaerobic *E. coli* following the addition of HP [1-^{13}C]-pyruvate. Although metabolic fluxes from pyruvate to acetaldehyde in *S. cerevisiae*[12] and of pyruvate to formate in *E. coli*[13] have been recently measured using dDNP-enhanced ^{13}C NMR in vitro, close signal proximity or overlap between the metabolic products and their direct precursors complicated these measurements in vivo, where the resonances are often broader. For example, the close proximity of the relatively weak HP [1-^{13}C]acetaldehyde peak to the peak from its precursor, HP [2-^{13}C]pyruvate, prevented reliable assignment of the former resonance in a model using transgenic PDC from *Z. mobilis* (*zm*PDC) as a reporter gene for dDNP ^{13}C MR.[14] The present HP ^{1}H NMR study demonstrates that both spontaneous and INEPT-driven ^{13}C → ^{1}H polarization transfers provide a clear ^{1}H signature of these enzymatic processes. The usefulness of these experiments was further evaluated by comparisons against ^{13}C-detected dDNP NMR measurements.

2. MATERIAL AND METHODS

2.1. Pyruvate Decarboxylase (PDC) Preparation. A stock solution of *S. cerevisiae* pyruvate decarboxylase (Sigma) was prepared, containing approximately 90 units/mL with 1 mM Mg^{2+} and 25 μM thiamine pyrophosphate (TPP). Twelve units of this PDC stock solution were added to 50 mM citrate buffer, pH 6.0, supplemented with approximately 4 mM $MgCl_2$ and 2 mM TPP and maintained at 310 K for NMR experiments aimed at comparing INEPT-driven polarization transfer with spontaneous ^{13}C → ^{1}H transfers. One unit of the PDC stock solution dissolved in 100 mM phosphate buffer (pH 7.0) and maintained at 293 K was used for the kinetic measurements. Per definition, one unit of PDC converts 1 μmol of pyruvate to acetaldehyde per minute at 298 K and pH 6.0; it would therefore catalyze a steady state flux of approximately 16.7 nmol s^{-1} or ca. 28 μM s^{-1} for the 600 μL volumes typically used in the experiments described here.[15]

2.2. Media and Growth Conditions. Optical densities were measured at 600 nm (OD_{600}) using an Ultrospec 10 (Amersham Biosciences, Cambridge, UK) cell density meter. Cultures of the *S. cerevisiae* strain BY4743 were grown in yeast extract peptone dextrose (YPD) medium in an orbital incubator (MRC Ltd., Holon, Israel) at 200 rpm and 30 °C. For the NMR experiments batch cultures of 150 mL of YPD, inoculated from overnight starter cultures to an $OD_{600} \approx 0.10$, were grown to midexponential phase. A 25 mL sample of this culture ($OD_{600} = 2.10$) was then harvested by centrifugation for 5 min at 6000*g* and room temperature. The supernatant was discarded, the pellet was resuspended in 5 mM sodium acetate buffer in 0.9% saline solution (pH = 4.5), and the cells were then centrifuged again for 5 min at 6000, resuspended in 40 mM HCl−KCl buffer (pH = 2.0), and immediately used in MR experiments.

Cultures of the *E. coli* strain MG1655 were inoculated from an agar plate into 10 mL of LB Lenox medium and grown overnight in an orbital incubator at 200 rpm and 37 °C. The next day a starter culture was used to inoculate a Bioflo 110 fermenter (New Brunswick Scientific, Enfield, CT) containing 900 mL of M9ZB medium (6 g/L Na_2HPO_4, 3 g/L KH_2PO_4, 5 g/L NaCl, 1g/L NH_4Cl, 0.25 g/L $MgSO_4{\cdot}7H_2O$, 10 g/L casein peptone, and 5 mg/L vitamin B1, pH = 7.1) supplemented with 0.2% sodium pyruvate and 0.2% glucose. The culture was grown in batch mode at 37 °C with continuous mixing at 250 rpm. Anaerobic conditions were maintained by bubbling a 9:1 mixture of nitrogen and carbon dioxide through the culture at 2.7 L/min. A 20 mL sample of the culture grown to midexponential phase ($OD_{600} = 2.60$) was centrifuged at room temperature for 5 min at 6000*g*. The supernatant was discarded, and the cell pellet was

DOI: 10.1021/jacs.6b07483
J. Am. Chem. Soc. 2016, 138, 12278−12286

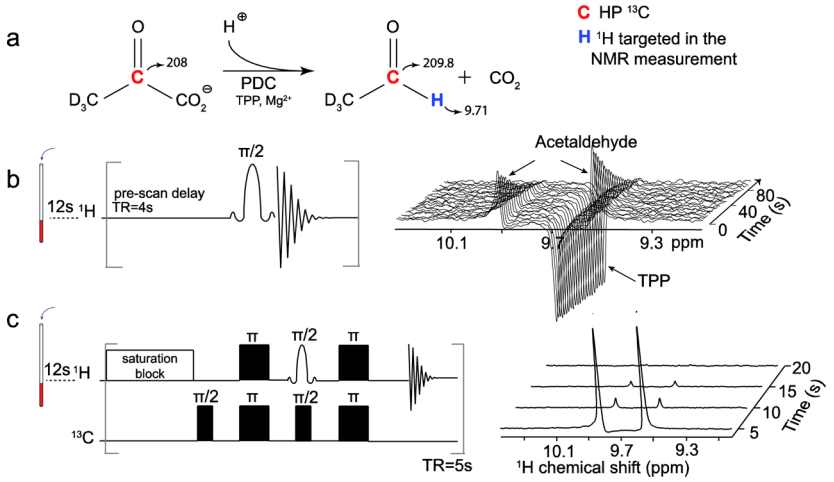

Figure 1. ^{1}H dDNP NMR measurements of PDC activity. (a) Reaction catalyzed by PDC, showing the ^{13}C and ^{1}H NMR chemical shifts (in ppm) of the indicated nuclei. (b) ^{13}C-enhanced ^{1}H acquisitions resulting from the application of a 90°-shaped pulse centered on the acetaldehyde proton resonance. The right-hand panel shows an array of 22 spectra acquired after the addition of HP [2-^{13}C]pyruvate (TR = 4 s). A thermally polarized TPP cofactor resonance appears with opposite phase.[11a] (c) Spectra acquired under the same conditions as in b but using the reverse INEPT pulse sequence shown on the left (TR = 5 s). All acquisitions started 12 s after the addition of 50 mM HP sodium [U-^{2}H$_3$,2-^{13}C]pyruvate to samples of the purified enzyme (12 U PDC in 50 mM citrate buffer, pH = 6.0, 310 K).

resuspended in 40 mM HEPES buffer, pH 7.4, and immediately used in MR experiments.

2.3. Dissolution Dynamic Nuclear Polarization. For dDNP, 40 mg of sodium [U-^{2}H$_3$,2-^{13}C]pyruvate (see Supporting Information 1 for deuterium enrichment of commercially available sodium [2-^{13}C]-pyruvate) was dissolved in 60 μL of D_2O and mixed with 40 μL of a solution containing 37.5 mM of Ox063 trityl radical (GE Healthcare, Little Chalfont, UK) dissolved in anhydrous glycerol. Gadoteric acid (DOTAREM; Guebert, Roissy, France) was then added to a final concentration of 15 mM. [U-^{2}H$_3$,2-^{13}C]pyruvic acid or [1-^{13}C]pyruvic acid was hyperpolarized by dissolving Ox063 to 15 mM in neat solutions of these self-glassing metabolites. These solutions were cooled to 1.3 K and polarized in a 3.35 T Hypersense (Oxford Instruments, Abingdon, UK) using 100 mW microwaves at the appropriate frequencies. After approximately 120−150 min of irradiation, the samples were rapidly dissolved in buffers that had been preheated to 180 °C and pressurized to 10 bar. These dissolution buffers included 50 mM citrate at pH = 6.0 or 100 mM sodium phosphate buffer for experiments with purified PDC (see below), 40 mM HCl−KCl buffer at pH 2.0 for experiments with *S. cerevisiae* cell suspensions, and 40 mM HEPES containing NaOH for experiments with *E. coli* cell suspensions. Approximately 500 μL of the dissolved samples was injected into the NMR tube containing either PDC or the cell suspensions. An automatic device for sample transfer using gradients of gas pressure[16,17] was employed to deliver a reliably preset volume of the HP sample into a NMR tube, which had been preloaded with the enzyme solution or cell suspension to be analyzed and placed inside the NMR magnet. This Arduino-controlled device effectively prevented bubble formation in the sample, and allowed NMR measurements on thoroughly mixed sample solutions to begin with high reproducibility as early as 3 s after dissolution. The final concentration of HP [U-^{2}H$_3$,2-^{13}C]pyruvate was 15 or 6 mM for the in vitro PDC experiments, 6 mM [U-^{2}H$_3$,2-^{13}C]pyruvic acid for the *S. cerevisiae* experiments, and 6 mM [1-^{13}C]pyruvate for the *E. coli* experiments.

2.4. NMR Spectroscopy. An 11.7 T (500 MHz ^{1}H) Inova medium-bore NMR spectrometer (Varian, Palo Alto, CA) equipped with a 5 mm triple-resonance HCN NMR inverse probe with *x*−*y*−*z* gradients or with a single-gradient 5 mm double-resonance direct-detect HX probe, were used for the ^{1}H and ^{13}C NMR measurements, respectively. ^{1}H NMR spectra were acquired using a 3-lobed *sinc* pulse exciting an 800 Hz bandwidth and centered at the ^{1}H frequency of either the acetaldehyde or the formate resonance (9.71 or 8.44 ppm, respectively) targeted depending on the experiment. These *sinc* pulses were tuned to give 90° nutations when comparing the efficiencies of the spontaneous vs the INEPT transfers in the in cell experiments or to 30° nutations when performing the kinetic measurements. For the spontaneous transfer experiments repetition times (TR) were set to 3 or 4 s, as specified below. INEPT spectra were recorded by transferring the ^{13}C hyperpolarization to the ^{1}H of acetaldehyde using a reversed refocused INEPT sequence[18] based on a J_{CH} = 177 Hz. This coupling constant was measured independently by ^{1}H NMR on a 1.0 M acetaldehyde solution in 50 mM sodium citrate buffer. *Sinc*-shaped ^{1}H selective pulses were also used in these INEPT experiments with a TR = 5 s. To ensure full suppression of both water and nonhyperpolarized ^{1}H background, a gradient-based saturation block of 90°−180°−180° ^{1}H pulses followed by triaxial gradient pulses (5 ms) with different directions and intensities, was applied before the polarization transfer process. dDNP ^{13}C spectra were acquired using a single transient pulse/acquire experiment with a 12° flip angle pulse and TR = 3 s. In addition, ^{1}H NMR spectra of midexponential phase *E. coli* cell samples were collected 5 min after the addition of thermally polarized [1-^{13}C]pyruvate; these were acquired using a 4 s, on-resonance water presaturation pulse during the relaxation delay, 90° pulses, and 64 transients.

NMR spectra were obtained by weighting the time-domain signals with a 1−10 Hz apodization filter for the ^{1}H acquisitions and a 1 Hz apodization for the ^{13}C acquisitions followed by Fourier transformation and phasing. All these procedures were performed using custom-written Matlab routines (The Mathworks Inc., Nantucket, USA).

3. RESULTS

3.1. Characterizing PDC Activity by ^{1}H NMR. PDC catalyzes the first reaction in the two-step pyruvate → acetaldehyde → ethanol conversion (Figure 1a). The latter step—the reduction of acetaldehyde to ethanol and reoxidation of NADH—is catalyzed by alcohol dehydrogenase and regenerates NAD^+, an electron acceptor essential in the early steps of glycolysis.[19] As the ^{13}C chemical shift difference between [2-^{13}C]pyruvate and [2-^{13}C]acetaldehyde is less than 2 ppm, detection of this reaction in vivo by ^{13}C dDNP NMR has been challenging.[20] By contrast, the new ^{1}H resonance arising at ∼9.7 ppm as a result of pyruvate decarboxylation is readily detectable, as confirmed by injection of hyperpolarized [U-^{2}H$_3$,2-^{13}C]pyruvate into solutions of purified PDC from *S.*

DOI: 10.1021/jacs.6b07483
J. Am. Chem. Soc. 2016, 138, 12278−12286

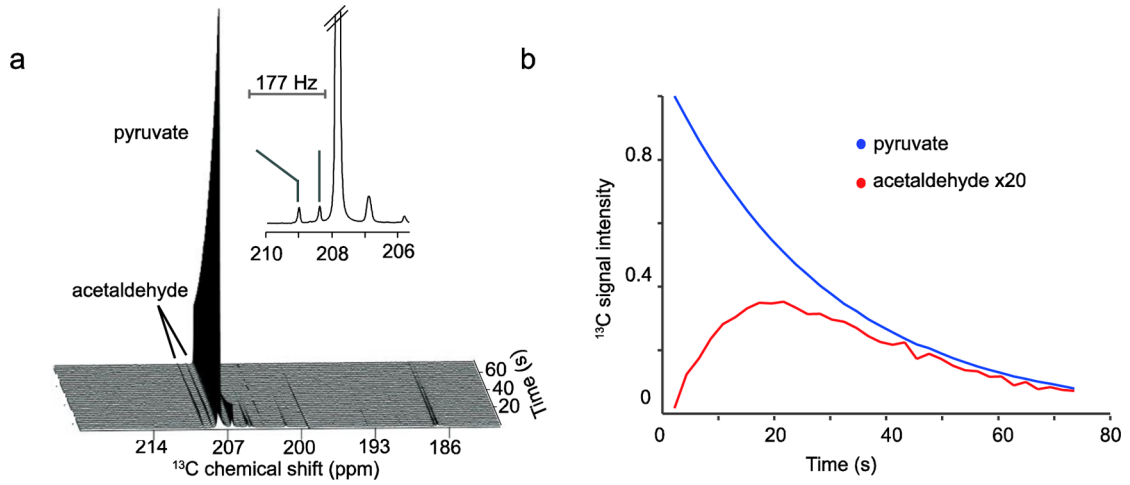

Figure 2. In vitro ^{13}C NMR measurements of PDC activity. Spectra were acquired ca. 1 s after the rapid addition of 6 mM HP [U-$^{2}H_3$,2-^{13}C]pyruvate to a sample of purified enzyme (2 U PDC in 50 mM citrate buffer, pH = 6.0, 310 K). (a) Array of 34 ^{13}C spectra collected with TR = 2.2 s; (inset) pyruvate/acetaldehyde carbonyl resonances in the summed spectra, with a marker indicating the J_{CH} splitting in acetaldehyde. (b) Time dependence of the integrated pyruvate and acetaldehyde ^{13}C signal intensities, normalized to the maximum pyruvate signal (the acetaldehyde signal intensity was multiplied by 20×).

cerevisiae. ^{1}H NMR spectra recorded using a shaped 90° excitation centered on the acetaldehyde resonance show a substantially enhanced ^{1}H signal. This signal arises from [1-^{1}H, 2,2,2-$^{2}H_3$,1-^{13}C]acetaldehyde (Figure 1b) due to a spontaneous $^{13}C \rightarrow {}^{1}H$ polarization enhancement from the hyperpolarized precursor and appears split due to a J_{CH} = 177 Hz coupling with the ^{13}C. A ^{1}H peak arising from TPP's thiazole ring is also detectable due to the relatively high (2 mM) concentration of the cofactor in this experiment. This peak possesses an opposite phase as the acetaldehyde resonances due to our choice of hyperpolarizing the pyruvate at $\omega_e - \omega_c$, which leads to antipolarization of the ^{1}H nucleus. Moreover, the TPP signal remains constant over time, while the acetaldehyde ^{1}H intensity decays into the noise background due to it's progressive loss of hyperpolarization. Indeed, no acetaldehyde ^{1}H signal could be observed on this time scale when using a thermally polarized substrate (data not shown). Notice that despite our use of 90° excitation pulses, the DNP-enhanced single-shot ^{1}H signal is observable for over 80 s; this is much longer than the usual T_1^H and reflects a signal decay dictated by the T_1 of the ^{13}C. Notice as well the unequal intensity of the *J*-coupled doublet, reflecting the effects of the cross-correlated dipolar/chemical-shift anisotropy relaxation driving the spontaneous $^{13}C \rightarrow {}^{1}H$ polarization transfer.[11] Repetition of this experiment using a reversed INEPT sequence transferring polarization from the ^{13}C to the ^{1}H via *J* couplings (Figure 1c) leads to a substantially higher SNR when compared to the spontaneous polarization transfer: SNRs of 195 and 15 are observed for the first ^{1}H scans of these acquisitions, respectively. However, while INEPT transfers the full [1-^{13}C]acetaldehyde polarization in one shot, the cross-relaxation effect enables the detection of an enhanced ^{1}H signal over numerous repetitions (Figure 1b). Kinetic results are also available from dDNP ^{13}C NMR, whose spectra show the build-up and decay of the acetaldehyde signal starting 3 s after injection of 6 mM HP [U-$^{2}H_3$,2-^{13}C]pyruvate (Figure 2). The slow decay of this resonance is consistent with the spontaneous $^{13}C \rightarrow {}^{1}H$ polarization transfer shown in Figure 1b. Note that although the pyruvate 2-^{13}C resonance can be distinguished from its ^{1}H-coupled [1-^{13}C]acetaldehyde counterpart in this in vitro ^{13}C NMR experiment, such resolution will not generally be achievable in vivo.[14] No such limitation arises for the ^{1}H-based detections.

The cross-relaxation-driven ^{1}H-detected experiments enabled the acquisition of time-resolved spectroscopic data displaying both a build-up and a decay of the acetaldehyde signals (Figure 1b). In the set of experiments illustrated in Figure 3, HP [U-$^{2}H_3$,2-^{13}C]pyruvate was injected automatically at two different concentrations (15 and 6 mM) into separate samples containing 1 unit of PDC activity. The acetaldehyde ^{1}H resonance showed a signal build up for ca. 20 s, followed by ∼100 s of signal decay (Figure 3b, blue trace). The maximum intensity of the acetaldehyde signal in the experiment using 15 mM pyruvate was observed approximately 8 s earlier than the maximum recorded with 6 mM pyruvate. This may reflect changes in the T_1s of the various chemical species upon changing the amount of injected HP pyruvate preparation, as these changes would also alter the concentration of the radical and thereby the metabolites' relaxivities (Figure S2).[21] The acetaldehyde ^{1}H signal kinetics can be modeled using equations derived from the Bloch−McConnell formalism of chemical exchange.[22] This signal intensity will depend on its rate of production from [1-^{13}C]acetaldehyde via a $^{13}C \rightarrow {}^{1}H$ cross-relaxation process occurring at a rate constant $k_{x\text{-}rel}$ and on dissipative processes arising from T_1^H relaxation and from repetitively exciting the ^{1}H polarization. At the same time the [1-^{13}C]acetaldehyde polarization will increase due to the irreversible conversion of [2-^{13}C]pyruvate into acetaldehyde at a rate k_{pdc} determined by the kinetic properties of PDC. The ^{13}C magnetizations of [2-^{13}C]pyruvate and [1-^{13}C]acetaldehyde will in turn decay at rates determined by their individual T_1^Cs but will not be depleted by excitation. Referring to $M_z^{C,pyr}$, $M_z^{C,acet}$, and $M_z^{H,acet}$ as the magnetizations of the species just alluded, given by the products of their respective polarizations and concentrations, the effects of these rates on the NMR signals can be described as

$$\frac{dM_z^{C,pyr}}{dt} = -\frac{M_z^{C,pyr}}{T_1^{C,pyr}} - k_{pdc} \cdot M_z^{C,pyr} \quad (1)$$

DOI: 10.1021/jacs.6b07483
J. Am. Chem. Soc. 2016, 138, 12278−12286

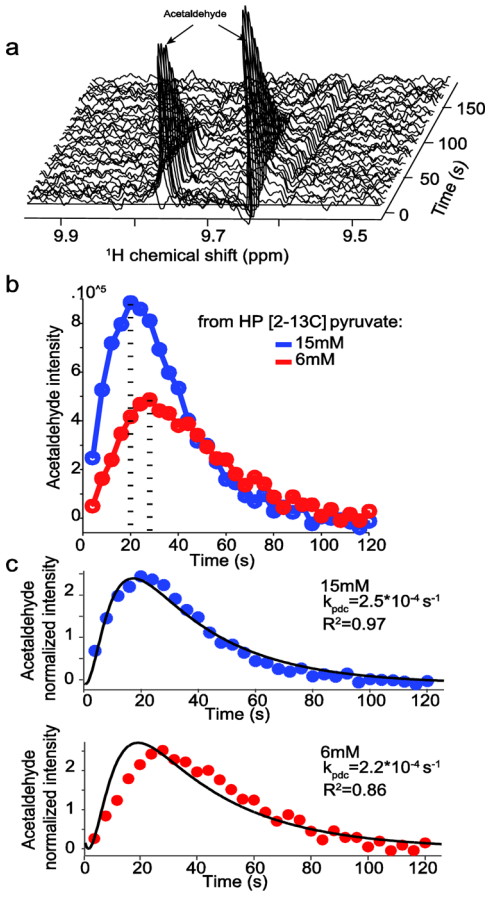

Figure 3. ^{1}H NMR measurements of k_{pdc}, the apparent rate constant describing the conversion of pyruvate to acetaldehyde catalyzed by PDC. Spectra were acquired using 30°-shaped ^{1}H pulses, following addition of HP [U-^{2}H$_3$,2-^{13}C]pyruvate to a sample containing purified PDC (1 unit in 100 mM phosphate buffer, pH = 7.0, 293 K). (a) Array of 40 ^{1}H NMR spectra (TR = 4 s) acquired following the addition of 15 mM ^{13}C-hyperpolarized pyruvate. (b) Integrated intensity of the ^{1}H acetaldehyde signal after injection of 15 (blue) and 6 mM (red) HP [U-^{2}H$_3$,2-^{13}C]pyruvate. Dashed lines show the maximal acetaldehyde signal intensities. (c) Fits (solid lines) of the integrated acetaldehyde signal intensities (symbols), normalized to the total thermal signal acquired 30 min after the injection, obtained following addition of 15 (top) and 6 mM (bottom) hyperpolarized [U-^{2}H$_3$,2-^{13}C]pyruvate. Fits were obtained as described in the text (see Supporting Information 2 for further details).

$$\frac{dM_z^{C,acet}}{dt} = -\frac{M_z^{c,acet}}{T_1^{c,acet}} + k_{pdc}\cdot M_z^{C,pyr} - k_{x-rel}M_z^{C,acet} \quad (2)$$

$$\frac{dM_z^{H,acet}}{dt} = k_{x-rel}\cdot M_z^{C,acet} - \frac{M_z^{H,acet}}{T_1^{H,acet}} - \frac{(1-\cos\theta)}{TR}\cdot M_z^{H,acet} \quad (3)$$

Here θ is the ^{1}H excitation pulse angle, TR is the repetition time, and $T_1^{c,pyr}$, $T_1^{c,acet}$, and $T_1^{H,acet}$ are the longitudinal relaxation times of [2-^{13}C]pyruvate, [1-^{13}C]acetaldehyde, and [1-^{1}H]-acetaldehyde, respectively. With these parameters and setting $M_z^{C,pyr}(t=0) = \text{Polarization}_{Pyr} \times [Pyr]_0$, $M_z^{C,acet}(t=0) = 0$ and $M_z^{H,acet}(t=0) = 0$ as the initial starting conditions, these differential equations were solved for k_{pdc} as a function of $[Pyr]_0$. The ^{13}C relaxation times of [2-^{13}C]pyruvate and [1-^{13}C]acetaldehyde following the injection of 6 mM HP pyruvate were assumed to be equal to those measured previously under similar conditions but in the absence of the Ox063 trityl radical. These previous measurements gave T_1's of 29.5 and 11.5 s, respectively.[14] The acetaldehyde 1-^{1}H T_1 was estimated to be 5.0 s, and $k_{x\text{-}rel}$ was set to 0.1 Hz on the basis of previous observations of this phenomenon in small molecules.[11]

A closed form solution of eqs 1−3 (see Supporting Information 2) indicates that even with all relaxation parameters known, fitting the HP ^{1}H-acetaldehyde signal intensities over time can only provide the $k_{pdc} \times M_z^{C,pyr}(t=0)$ product. Figure 3c shows the resulting kinetic analyses of the acetaldehyde ^{1}H signal evolution at two different substrate concentrations, where the acetaldehyde signal was normalized to the thermal signal recorded using a 90°-shaped pulse 30 min after the HP substrate injection. Assuming that this long-term thermal ^{1}H signal is proportional to the initial pyruvate concentration, this should eliminate the $[Pyr]_0$ parameter from the fitting of $k_{pdc} \times M_z^{C,pyr}$. The data then reveal a 14% increase in the $k_{pdc} \times M_z^{C,pyr}(t=0)$ term upon increasing $[Pyr]_0$ from 6 to 15 mM. Assuming that in these measurements the polarization enhancement at the time of injection into the NMR tube was constant between experiments and on the order of ∼8000× the thermal signal, the apparent initial first-order rate constant, k_{pdc}, describing the conversion of pyruvate to acetaldehyde can then be estimated to be 2.2 × 10^{-4} s^{-1} at 6 mM and 2.5 × 10^{-4} s^{-1} at 15 mM HP pyruvate, respectively. With these assumptions the enzymatic flux ($k_{pdc} \times$ [pyruvate]) can be estimated, giving 1.3 and 3.8 μM s^{-1} at the initial HP pyruvate concentrations of 6 and 15 mM, respectively.

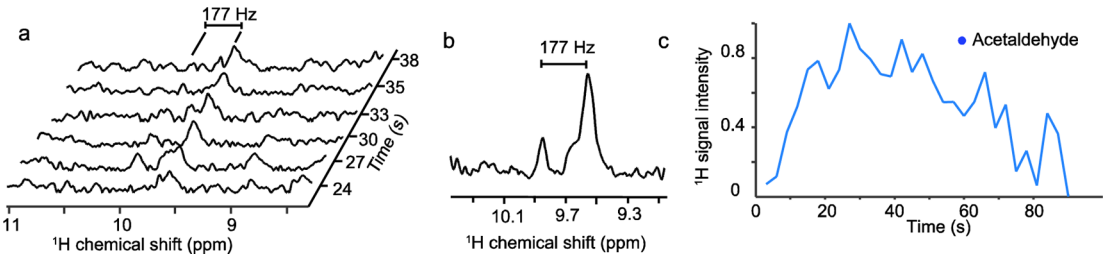

Figure 4. ^{1}H NMR measurements of acetaldehyde production in a sample from a midexponential phase *S. cerevisiae* culture. (a) ^{1}H spectra acquired starting 24 s after the addition of 6 mM HP [U-^{2}H$_3$,2-^{13}C]pyruvic acid in HCl−KCl buffer, pH = 2.0, using a 90° acetaldehyde-selective ^{1}H pulse, TR = 3 s. (b) Sum of the 6 spectra presented in a, showing a J doublet whose asymmetry originates in the cross-relaxation dynamics.[11a] (c) Time dependence of the integrated acetaldehyde doublet signal intensities, normalized to the maximum acetaldehyde signal; all measurements were made at 310 K.

DOI: 10.1021/jacs.6b07483
J. Am. Chem. Soc. 2016, 138, 12278−12286

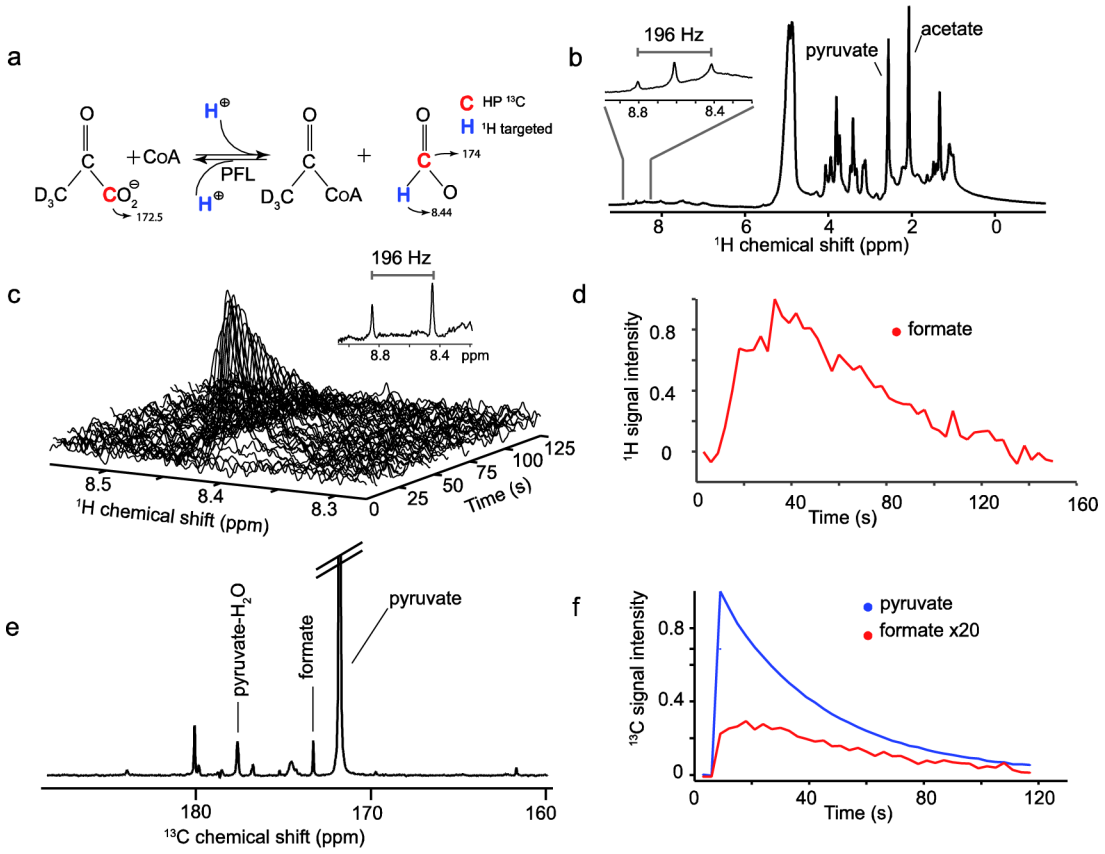

Figure 5. NMR measurements of formate production from [1-^{13}C]pyruvate in samples of midexponential phase *E. coli* cultures. (a) Reaction catalyzed by PFL, indicating the ^{13}C and ^{1}H NMR chemical shifts of the detected nuclei. CoA: coenzyme-A. (b) ^{1}H NMR spectrum of a sample from a midexponential phase culture of *E. coli*, acquired with water presaturation, 5 min after the addition of 6 mM thermally polarized [1-^{13}C]pyruvate. Methyl peaks of acetate and pyruvate are indicated, while the inset shows an expanded region containing the formate ^{1}H resonances. (c) Array of 40 ^{1}H NMR spectra acquired from the downfield formate ^{1}H peak following the addition of 6 mM HP [1-^{13}C]pyruvate using a selective (800 Hz bandwidth) 90° pulse, TR = 3 s. The inset, which shows the sum of the first 20 spectra, highlights the formate ^{1}H resonance split by the ^{13}C and asymmetric due to the ^{13}C → ^{1}H cross relaxation dynamics.[11a] (d) Time dependence of the integrated ^{1}H signal intensities from ^{13}C-formate. (e) Sum of the first 40 ^{13}C spectra acquired after addition of 6 mM HP [1-^{13}C]pyruvate to a sample of the bacterial cell culture; flip angle = 12°, TR = 3 s. (f) Time dependence of the integrated ^{13}C signal intensities from [1-^{13}C]pyruvate (blue) and [^{13}C]formate (red) in spectra acquired as described in c. Cultured cells were resuspended in 40 mM HEPES buffer, pH = 7.4 and maintained at 310 K throughout these measurements. Signals in d and f are shown normalized to their maximum intensities.

Reported substrate concentration/enzyme velocity relationships for PDC extracted from *S. cerevisiae* predict steady-state fluxes in the 6−18 μM s^{-1} range under similar conditions (100 mM inorganic phosphate concentration, pH = 6.0).[15] Given the differences between those extract experiments and the present dDNP runs, this represents a reasonable agreement between the flux values.

3.2. ^{1}H NMR Detection of PDC Activity in *S. cerevisiae* Cell Suspensions. ^{1}H-based measurements of PDC activity using HP [U-^{2}H$_3$,2-^{13}C]pyruvate were also explored in intact *S. cerevisiae* cells. Cells were harvested by centrifugation (10 min at 5000*g*) at midexponential phase growth and incubated in 5 mM acetate buffer in 0.9% saline (pH = 4.5) solution for 10 min; they were then reharvested and resuspended in KCl−HCl buffer (pH 2.0), and the production of [1-^{1}H, 2,2,2-^{2}H$_3$,1-^{13}C]-acetaldehyde was observed by ^{1}H NMR following the addition of 6 mM HP [U-^{2}H$_3$,2-^{13}C]pyruvic acid. Figure 4 shows representative spectra acquired from these cell suspensions for approximately 1 min following substrate injection using selective 90° ^{1}H pulses (TR = 3 s). In experiments with thermally polarized pyruvate and natural abundance ^{13}C this ^{1}H signal appeared transiently approximately 2−3 min after substrate addition, but no signals were observed on the initial-rate time scale of the dDNP experiments (data not shown).

3.3. ^{1}H NMR Detection of PFL Activity in Intact *E. coli*. The production of [^{13}C]formate from HP [1-^{13}C]pyruvate catalyzed by pyruvate formate lyase (PFL, Figure 5a) can also be conveniently detected via transfer of polarization from hyperpolarized ^{13}C to ^{1}H. PFL activity is essential under anaerobic conditions, as reflected by the >12-fold increase in its expression and increased post-translational activation in anoxia.[23] The acetyl-CoA produced by PFL can be further metabolized to ethanol or acetate, reoxidizing NADH to NAD^{+}, thus helping to maintain redox balance or increasing ATP yield, respectively.[24] The second product of this enzyme, formic acid, can be slowly metabolized further, depending on culture conditions; typically, however, it accumulates, together with ethanol and acetate, as the end product of glucose fermentation.[24] The ^{1}H spectrum of *E. coli* recorded 5 min after the addition of thermally polarized 6 mM [1-^{13}C]pyruvate at pH = 7.4 (Figure 5b) displays three formate-related peaks: a doublet from [^{13}C]formate (with J_{CH} = 196 Hz) produced from the ^{13}C-labeled pyruvate and a singlet from [^{12}C]formate

DOI: 10.1021/jacs.6b07483
J. Am. Chem. Soc. 2016, 138, 12278−12286

produced from carbon sources not enriched in ^{13}C. Formate production was also observed within seconds by the appearance of this downfield ^{1}H NMR doublet after addition of 6 mM hyperpolarized [1-^{13}C]pyruvate to a sample of *E. coli* cells from a midexponential phase culture (Figure 5c). The increased sensitivity resulting from hyperpolarization allowed PFL activity to be measured in these intact cells (Figure 5d). Again, the ^{1}H polarization enhancement persisted for a period that was well over an order of magnitude longer than the T_1^H. The clear resolution of these ^{1}H resonances contrasted with the much poorer resolution of the ^{13}C spectra, which showed overlap between the ^{13}C resonances of [^{13}C]formate and [1-^{13}C]-pyruvate (Figure 5e). The downfield peak of the formate doublet was detectable at δ = 174 ppm, while the upfield component (δ = 172.4 ppm) overlapped the pyruvate peak (δ = 172.5 ppm). Kinetic analysis based solely on the downfield ^{13}C resonance showed a maximum formate signal intensity at ~20 s after pyruvate injection (Figure 5f) as compared to a peak at ~40 s when formate was detected via the ^{1}H spectrum (Figure 5d). This faster apparent rate in the directly detected ^{13}C experiment when compared to the indirectly detected ^{1}H experiment reflects the different T_1's of the reactant and products, as can be appreciated by the simulated evolutions shown in Figure S3.

4. DISCUSSION

While dDNP has been used mainly with direct detection of hyperpolarized ^{13}C- or ^{15}N-labeled metabolites,[20,25,26] the present work investigated the potential of detecting a hyperpolarized ^{13}C label via its transfer to ^{1}H. Enhancement of the ^{1}H signal via ^{13}C polarization transfer overcomes a main limitation of hyperpolarized ^{1}H MR: namely, short ^{1}H T_1s. In general, owing to their larger spectral dispersion and narrower spectral lines, ^{13}C NMR detection of hyperpolarized ^{13}C-labeled metabolites should be more useful than ^{1}H detection. Furthermore, in contrast to ^{1}H NMR, ^{13}C NMR does not have to deal with background signals from endogenous metabolites or with an intense water resonance. However, as demonstrated here, in some cases considerable advantages can result from transferring hyperpolarization from ^{13}C to ^{1}H and then detecting the latter. In the specific examples shown, observing the ^{1}H signals of labeled acetaldehyde and formate eliminated ^{13}C spectral overlap problems between the precursors and the products in these reactions. Indeed, while the [1-^{13}C]-acetaldehyde doublet could be resolved from [2-^{13}C]pyruvate signal at high magnetic field in vitro (Figure 2a and ref 12), reliable assignment of the former resonance was difficult in in vivo MR experiments, which typically have wider lines.[14] Even more challenging becomes then the selective excitation of the products while preserving the reactant's hyperpolarization, as is often desirable in HP NMR. Consequently, ^{1}H-based detection may better suit the measurement of flux in these reactions. We further confirmed this with in vivo experiments on cells expressing a transgenic *zm*PDC reporter gene, whose metabolism could be followed by ^{1}H NMR but not via ^{13}C when HP [2-^{13}C]pyruvate was used as substrate (see Supporting Information 3 and ref 14 for further details).

Heteronuclear $^{13}C \rightarrow {}^{1}H$ polarization transfers had been previously exploited in static $^{13}C-{}^{1}H$ pairs, devoid of chemical conversions.[9a−f,11,27] This study demonstrates that the same mechanisms can be used to enhance the ^{1}H signals of metabolic products produced in situ in either test tubes or intact cells. In the enzymatic reactions studied here, the formation of new covalent bonds between the hyperpolarized ^{13}C nucleus and ^{1}Hs in both acetaldehyde and formate allowed us to transfer hyperpolarization by either *J*-driven sequences or by spontaneous cross-relaxation. Features favoring the execution of such reversed INEPT experiments include (i) the possibility to transfer HP between heteronuclei multiple bonds away,[9c−g,27] something that cross-relaxation would be very inefficient at doing, (ii) the possibility of incorporating coherence-selection field gradients to efficiently eliminate background ^{1}H signal of endogenous metabolites (as illustrated by the absence of the pronounced TPP signal present in the conventional ^{1}H spectrum, Figure 1b), and (iii) the possibility of delivering ^{1}H NMR spectra with approximately an order of magnitude greater SNR than those achieved via the cross-relaxation effect, which can be seen by comparing Figure 1b and 1c. Further, neither ^{1}H NMR enhanced by cross-relaxation nor direct ^{13}C detection using a low flip angle excitation allowed detection of the activity of transgenic *zm*PDC expressed by HEK293T cells in vitro (data not shown). ^{1}H-detected INEPT, however, allowed detection of the acetaldehyde produced from the injected HP pyruvate (Figure S1). This strong signal enhancement achieved by the reversed INEPT experiment comes in part at the expense of depleting all of the ^{13}C polarization in a single acquisition. Lower amounts of polarization transfer can be delivered by the INEPT sequence;[9d,10] however, complex procedures are then needed to avoid waste of the hyperpolarization. A possible route to preserve the bulk ^{13}C hyperpolarization while using INEPT could also involve relying on sequences that selectively excite the product ^{13}C while carefully avoiding excitation of the reactant ^{13}C resonance(s); to our knowledge this approach has not yet been demonstrated in vivo.

On the other hand, as in the spontaneous transfer the HP ^{13}C is not excited, the enhanced ^{1}H signal can be acquired repeatedly over a time period governed by T_1^C rather than by T_1^H. This allowed us to quantify acetaldehyde's formation from pyruvate, as catalyzed by PDC. ^{1}H NMR spectra were then modeled using simple kinetics to extract k_{pdc}, the first-order rate constant describing this process (Figure 3). Phosphate buffer (100 mM) was used to increase the K_M of PDC for pyruvate,[15] which was added to initial concentrations of 6 and 15 mM. Decreasing the total PDC activity in the sample by reducing the amount of enzyme from 12 to 1 U and deviating slightly from the optimal pH (from pH = 6.0 to pH = 7.0[28]) eliminated the potential of substrate depletion during the experiment that could affect the level of enzyme saturation with the substrate. Still simulated evolutions of the pyruvate and acetaldehyde magnetizations (not shown) revealed that under conditions affording maximum PDC activity, the parameter limiting the ^{1}H acetaldehyde signal formation will be the rate of polarization transfer: under optimal conditions k_{pdc} is simply too fast vis-à-vis $k_{x\text{-}rel}$ to reveal changes arising upon modulating substrate concentration.

Notably, the maximum acetaldehyde signal intensity in these experiments was recorded ~8 s earlier at an initial HP pyruvate concentration of 15 mM, in comparison to that recorded with 6 mM HP pyruvate (Figure 3). This did not reflect reproducibility issues, which were minimized by our use of an automatic sample transfer device, nor changes in k_{pdc}. Rather, it likely reflected changes in the T_1's of the species in chemical exchange, a consequence of the different final concentration of the polarizing radical between these experiments[21] (see Figure S1). Had all the NMR parameters been known, the kinetic

DOI: 10.1021/jacs.6b07483
J. Am. Chem. Soc. 2016, 138, 12278−12286

analysis would have delivered quantitative values for the enzymatic rate. While this knowledge was available for the relaxation and pulse parameters within fairly narrow ranges, the degree of ^{13}C hyperpolarization achieved during these measurements could only be estimated within a factor of ~2. Using a reasonable estimate of the ^{13}C hyperpolarization (8000×) the enzymatic flux was valued at 1.3 and 3.8 $\mu M\ s^{-1}$ at 6 and 15 mM HP pyruvate, respectively. These flux estimations are on the same order of magnitude as fluxes reported in the literature under slightly different conditions; moreover, their relative change upon increasing pyruvate concentration from 6 to 15 mM also compares very well with that predicted by the literature.[15] This confirms the usefulness of spontaneous $^{13}C \rightarrow {}^{1}H$ polarization transfers for real-time measurements of fast enzymatic reactions and fluxes.

The same process was explored in *S. cerevisiae*. Although these microorganisms can be grown on pyruvate as the sole source of carbon,[29] pyruvate does not permeate the plasma membrane during glucose fermentation.[30] Undissociated pyruvic acid, however, rapidly crosses the plasma membrane of glucose-fermenting *S. cerevisiae*.[30a] Consistent with this, a recent dDNP ^{13}C NMR study demonstrated rapid diffusion of undissociated HP [1-^{13}C]acetic acid into glucose-fermenting *S. cerevisiae*, a process which was favored by a low extracellular pH.[12] Once inside of the cell, pyruvic acid is rapidly decarboxylated by cytosolic PDC, a process which is pronounced during the exponential stages of cell growth.[30a] The product, acetaldehyde, is present in a low steady state concentration, and under normal physiological conditions it is rapidly reduced to ethanol. Acetaldehyde accumulation in *S. cerevisiae* cultures has been observed with acidification of the cytosol,[12] which has been attributed to inhibition of alcohol dehydrogenase combined with a shift in cytosolic pH to values closer to PDC's pH optimum of 6.0.[28,31] This is consistent with the experiments illustrated in Figure 4, where a relatively weak acetaldehyde ^{1}H signal was transiently observed in midexponential yeast cultures after incubation in acetate buffer at pH = 4.5 following exposure to HP pyruvic acid.

The wider applicability of spontaneous polarization transfer for investigating cell metabolism was demonstrated with *E. coli* investigations on the activity of PFL. PFL rapidly metabolizes pyruvate in anaerobic *E. coli* cultures, a process that is particularly pronounced when pyruvate is the main carbon source.[32] Flux of HP [^{13}C]glucose to [^{13}C]formate via [^{13}C]pyruvate has been measured with dDNP ^{13}C NMR at all growth phases of *E. coli* culture.[13] Consistent with these previous reports, we observed the rapid uptake and breakdown of pyruvate as a pronounced ^{1}H signal from formate (Figure 5c and 5d). In contrast to the relatively weak acetaldehyde signal detected in *S. cerevisiae* cultures after the addition of HP pyruvic acid (Figure 4), the build-up and decay of the formate signal could be observed on a single, scan-by-scan basis (Figure 5e). This higher SNR is explained by the rapid uptake of pyruvate and the accumulation of formate as a metabolic end product, characteristic of anaerobic *E. coli* cells. Further, the accumulation of acetaldehyde, a potent mutagen and cross-linking agent,[33] is generally prevented by its rapid metabolism within the cell. Consistent with this, measurements of ^{13}C flux between HP [1-^{13}C]ethanol and [1-^{13}C]acetate in mouse liver showed no evidence of the [1-^{13}C]acetaldehyde intermediate.[20] From the point of view of cell physiology, the significantly higher surface-to-volume ratio displayed by *E. coli* in comparison to *S. cerevisiae* and to human embryonic kidney cells would also be expected to facilitate a higher cell permeability to the substrate; this is consistent with the results shown here. Finally, the fact that pyruvate's $T_1^{C\text{-}1}$ is longer than its $T_1^{C\text{-}2}$ [14] may also have modestly contributed to the superior SNR obtained in the *E. coli* experiments.

5. CONCLUSIONS

This work showed that ^{13}C-based dDNP combined with spontaneous or *J*-driven polarization transfers can be used to monitor metabolic pathways in living cells by ^{1}H NMR. Although a similar potential based on ^{13}C NMR/MRI has already been demonstrated,[25] approaches based on ^{1}H detection may have advantages in terms of spectral resolution, better and more widely available detection hardware, and an increased sensitivity providing improvements in image resolution. The spontaneous transfer approach, in particular, enables the detection of hyperpolarized ^{1}H signals without demanding chemical manipulations of the probe immediately prior to the experiment[3,8b,27,34] or modifications of the original dissolution method.[6,7] All this could lead to a more widespread use of dDNP in a clinical setting, where hardware and sequences are optimized for ^{1}H imaging and where neither ^{13}C-tuned coils nor single or multichannel transceivers are typically available. A main challenge facing such in vivo extensions would arise from the need to carefully avoid being overwhelmed by the water peak; still, the fact that in many hydrogen-addition reactions the ensuing ^{1}H ends up resonating relatively far from 4.8 ppm could facilitate these selective observations despite the broad resonances usually arising in in vivo spectroscopy. Furthermore, while in the present study ^{13}C dDNP combined with INEPT produced substantially stronger ^{1}H signal enhancement than the spontaneous polarization transfer, the single-shot nature of magnetization transfer would likely make the former approach impractical for real-time measurements of metabolism in vivo. Finally, although the ^{13}C-enriched pyruvic acid used here as a HP probe is one of the most commonly used in vivo dDNP substrates,[35] other HP substrates capable of supporting similar phenomena can also be envisioned, including substrates that are hyperpolarized by methods other than DNP.

■ ASSOCIATED CONTENT

Supporting Information

The Supporting Information is available free of charge on the ACS Publications website at DOI: 10.1021/jacs.6b07483.

Deuterium enrichment procedure of sodium [U-$^{2}H_3$,2-^{13}C]pyruvate and [U-$^{2}H_3$,2-^{13}C]pyruvic acid; analytical solutions to the Bloch−McConnell differential equations describing the ^{13}C(substrate) → ^{13}C(product) → ^{1}H(product) polarization transfer kinetics; NMR experiments using HEK293T cells constitutively expressing zmPDC, containing Figure S1; figures describing the effects of kinetic parameters on the observed NMR signals in the process HP ^{13}C(substrate) → ^{13}C-(product) → ^{1}H(product) (PDF)

■ AUTHOR INFORMATION

Corresponding Author

*lucio.frydman@weizmann.ac.il

Author Contributions

§P.D. and A.F. contributed equally to this work.

DOI: 10.1021/jacs.6b07483
J. Am. Chem. Soc. 2016, 138, 12278−12286

Notes

The authors declare no competing financial interest.

■ ACKNOWLEDGMENTS

We are grateful to Dr. Veronica Frydman (WIS) and Christian Hundshammer (TUM) for the preparation of the [U-$^{2}H_{3}$,2-^{13}C]pyruvic acid. We acknowledge Dr. Christian Bretschneider (WIS) for his assistance in the use of the automatic sample injection device. Our research was supported by Israel Science Foundation grant 795/13, by the Kimmel Institute for Magnetic Resonance (Weizmann Institute), by DIP Project 710907, COST action TD-1113, and by the generosity of the Perlman Family Foundation. Work in the Brindle laboratory was supported by a Cancer Research UK Programme grant (17242) and by the CRUK-EPSRC Imaging Centre in Cambridge and Manchester (16465). The Schwaiger laboratory received funding from the European Union Seventh Framework Program (FP7) under Grant Agreement No. 294582, ERC Grant MUMI, and the Deutsche Forschungsgemeinschaft (DFG) under Grant Agreement No. SFB 824. A.F. gratefully acknowledges the French ministry of foreign affairs for an International Volunteers Program fellowship.

■ REFERENCES

(1) (a) Ardenkjaer-Larsen, J. H.; Fridlund, B.; Gram, A.; Hansson, G.; Lerche, M. H.; Servin, R.; Thaning, M.; Golman, K. *Proc. Natl. Acad. Sci. U. S. A.* **2003**, *100*, 10158−10163. (b) Griffin, R. G.; Prisner, T. F. *Phys. Chem. Chem. Phys.* **2010**, *12*, 5737−40. (c) Jeschke, G.; Frydman, L. *J. Magn. Reson.* **2016**, *264*, 1−2. (d) Kurhanewicz, J.; Vigneron, D. B.; Brindle, K.; Chekmenev, E. Y.; Comment, A.; Cunningham, C. H.; Deberardinis, R. J.; Green, G. G.; Leach, M. O.; Rajan, S. S.; Rizi, R. R.; Ross, B. D.; Warren, W. S.; Malloy, C. R. *Neoplasia* **2011**, *13*, 81−97.

(2) (a) Bowers, C. R.; Weitekamp, D. P. *Phys. Rev. Lett.* **1986**, *57*, 2645−2648. (b) Eisenschmid, T. C.; Kirss, R. U.; Deutsch, P. P.; Hommeltoft, S. I.; Eisenberg, R.; Bargon, J.; Lawler, R. G.; Balch, A. L. *J. Am. Chem. Soc.* **1987**, *109*, 8089−8091.

(3) Adams, R. W.; Aguilar, J. A.; Atkinson, K. D.; Cowley, M. J.; Elliott, P. I.; Duckett, S. B.; Green, G. G.; Khazal, I. G.; Lopez-Serrano, J.; Williamson, D. C. *Science* **2009**, *323*, 1708−11.

(4) Walker, T. G.; Happer, W. *Rev. Mod. Phys.* **1997**, *69*, 629−642.

(5) Levitt, M. H. *Spin Dynamics Basics of Nuclear Magnetic Resonance*; John Wiley and Sons Ltd.: Chichester, England, 2008.

(6) Harris, T.; Szekely, O.; Frydman, L. *J. Phys. Chem. B* **2014**, *118*, 3281−90.

(7) Ardenkjaer-Larsen, J. H.; Laustsen, C.; Bowen, S.; Rizi, R. *Magn. Reson. Med.* **2014**, *71*, 50−6.

(8) (a) Tayler, M. C. D.; Marco-Rius, I.; Kettunen, M. I.; Brindle, K. M.; Levitt, M. H.; Pileio, G. *J. Am. Chem. Soc.* **2012**, *134*, 7668−7671. (b) Bornet, A.; Ji, X.; Mammoli, D.; Vuichoud, B.; Milani, J.; Bodenhausen, G.; Jannin, S. *Chem. - Eur. J.* **2014**, *20*, 17113−8. (c) Canet, D.; Bouguet-Bonnet, S.; Aroulanda, C.; Reineri, F. *J. Am. Chem. Soc.* **2007**, *129*, 1445−9. (d) Kovtunov, K. V.; Truong, M. L.; Barskiy, D. A.; Koptyug, I. V.; Coffey, A. M.; Waddell, K. W.; Chekmenev, E. Y. *Chem. - Eur. J.* **2014**, *20*, 14629−32.

(9) (a) Donovan, K. J.; Frydman, L. *J. Magn. Reson.* **2012**, *225*, 115−119. (b) Frydman, L.; Blazina, D. *Nat. Phys.* **2007**, *3*, 415−419. (c) Giraudeau, P.; Shrot, Y.; Frydman, L. *J. Am. Chem. Soc.* **2009**, *131*, 13902. (d) Harris, T.; Giraudeau, P.; Frydman, L. *Chem. - Eur. J.* **2011**, *17*, 697−703. (e) Mishkovsky, M.; Frydman, L. *ChemPhysChem* **2008**, *9*, 2340−8. (f) Sarkar, R.; Comment, A.; Vasos, P. R.; Jannin, S.; Gruetter, R.; Bodenhausen, G.; Hall, H.; Kirik, D.; Denisov, V. P. *J. Am. Chem. Soc.* **2009**, *131*, 16014−5. (g) Ardenkjaer-Larsen, J. H.; Johannesson, H.; Petersson, J. S.; Wolber, J. *Methods Mol. Biol.* **2011**, *771*, 205−26.

(10) Norton, V. A.; Weitekamp, D. P. *J. Chem. Phys.* **2011**, *135*, 141107.

(11) (a) Donovan, K. J.; Lupulescu, A.; Frydman, L. *ChemPhysChem* **2014**, *15*, 436−442. (b) Merritt, M. E.; Harrison, C.; Mander, W.; Malloy, C. R.; Dean Sherry, A. *J. Magn. Reson.* **2007**, *189*, 280−285.

(12) Jensen, P. R.; Karlsson, M.; Lerche, M. H.; Meier, S. *Chem. - Eur. J.* **2013**, *19*, 13288−93.

(13) (a) Meier, S.; Jensen, P. R.; Duus, J. O. *FEBS Lett.* **2011**, *585*, 3133−8. (b) Meier, S.; Jensen, P. R.; Duus, J. O. *ChemBioChem* **2012**, *13*, 308−10.

(14) Dzien, P.; Tee, S. S.; Kettunen, M. I.; Lyons, S. K.; Larkin, T. J.; Timm, K. N.; Hu, D. E.; Wright, A.; Rodrigues, T. B.; Serrao, E. M.; Marco-Rius, I.; Mannion, E.; D'Santos, P.; Kennedy, B. W.; Brindle, K. M. *Magn. Reson. Med.* **2016**, *76*, 391−401.

(15) Boiteux, A.; Hess, B. *FEBS Lett.* **1970**, *9*, 293−296.

(16) Katsikis, S.; Marin-Montesinos, I.; Pons, M.; Ludwig, C.; Günther, U. L. *Appl. Magn. Reson.* **2015**, *46*, 723−729.

(17) Bowen, S.; Hilty, C. *Phys. Chem. Chem. Phys.* **2010**, *12*, 5766−70.

(18) Morris, G. A.; Freeman, R. *J. Am. Chem. Soc.* **1979**, *101*, 760−762.

(19) Pronk, J. T.; Yde Steensma, H.; Van Dijken, J. P. *Yeast* **1996**, *12*, 1607−1633.

(20) Dzien, P.; Kettunen, M.; Marco-Rius, I.; Serrao, E. M.; Rodrigues, T. B.; Larkin, T. J.; Timm, K. N.; Brindle, K. M. *Magn. Reson. Med.* **2015**, *73*, 1733−40.

(21) Chattergoon, N.; Martínez-Santiesteban, F.; Handler, W. B.; Ardenkjær-Larsen, J. H.; Scholl, T. J. *Contrast Media Mol. Imaging* **2013**, *8*, 57−62.

(22) McConnell, H. M. *J. Chem. Phys.* **1958**, *28*, 430−431.

(23) (a) Sawers, G.; Bock, A. *J. Bacteriol.* **1988**, *170*, 5330−6. (b) Nnyepi, M. R.; Peng, Y.; Broderick, J. B. *Arch. Biochem. Biophys.* **2007**, *459*, 1−9.

(24) Wang, Q.; Ou, M. S.; Kim, Y.; Ingram, L. O.; Shanmugam, K. T. *Appl. Environ. Microbiol.* **2010**, *76*, 2107−14.

(25) Day, S. E.; Kettunen, M. I.; Gallagher, F. A.; Hu, D. E.; Lerche, M.; Wolber, J.; Golman, K.; Ardenkjaer-Larsen, J. H.; Brindle, K. M. *Nat. Med.* **2007**, *13*, 1382−7.

(26) (a) Cudalbu, C.; Comment, A.; Kurdzesau, F.; van Heeswijk, R. B.; Uffmann, K.; Jannin, S.; Denisov, V.; Kirik, D.; Gruetter, R. *Phys. Chem. Chem. Phys.* **2010**, *12*, 5818−23. (b) Hata, R.; Nonaka, H.; Takakusagi, Y.; Ichikawa, K.; Sando, S. *Chem. Commun.* **2015**, *51*, 12290−2. (c) Jiang, W.; Lumata, L.; Chen, W.; Zhang, S.; Kovacs, Z.; Sherry, A. D.; Khemtong, C. *Sci. Rep.* **2015**, *5*, 9104.

(27) Chekmenev, E. Y.; Norton, V. A.; Weitekamp, D. P.; Bhattacharya, P. *J. Am. Chem. Soc.* **2009**, *131*, 3164−5.

(28) Sergienko, E. A.; Jordan, F. *Biochemistry* **2001**, *40*, 7369−81.

(29) Fendt, S.-M.; Sauer, U. *BMC Syst. Biol.* **2010**, *4*, 1−11.

(30) (a) Suomalainen, H.; Nurminen, T. *J. Inst. Brew.* **1976**, *82*, 218−225. (b) Foulkes, E. C. *J. Gen. Physiol.* **1955**, *38*, 425−30.

(31) Verduyn, C.; Postma, E.; Scheffers, W. A.; Van Dijken, J. P. *Yeast* **1992**, *8*, 501−17.

(32) (a) Lang, V. J.; Leystra-Lantz, C.; Cook, R. A. *J. Bacteriol.* **1987**, *169*, 380−5. (b) Kreth, J.; Lengeler, J. W.; Jahreis, K. *PLoS One* **2013**, *8*, e67125.

(33) Langevin, F.; Crossan, G. P.; Rosado, I. V.; Arends, M. J.; Patel, K. J. *Nature* **2011**, *475*, 53−8.

(34) (a) Barskiy, D. A.; Kovtunov, K. V.; Koptyug, I. V.; He, P.; Groome, K. A.; Best, Q. A.; Shi, F.; Goodson, B. M.; Shchepin, R. V.; Coffey, A. M.; Waddell, K. W.; Chekmenev, E. Y. *J. Am. Chem. Soc.* **2014**, *136*, 3322−5. (b) Pravdivtsev, A. N.; Yurkovskaya, A. V.; Petrov, P. A.; Vieth, H.-M.; Ivanov, K. L. *Appl. Magn. Reson.* **2016**, *47*, 711−725.

(35) Nelson, S.; Kurhanewicz, J.; Vigneron, D.; Larson, P. E. Z.; Harzstark, A. L.; Ferrone, M.; van Criekinge, M.; Chang, J. W.; Bok, R.; Park, I.; Reed, G.; Carvajal, L.; Small, E. J.; Munster, P.; Weinberg, V. K.; Ardenkjaer-Larsen, J. H.; Chen, A. P.; Hurd, R. E.; Odegardstuen, L.-I.; Robb, F. J.; Tropp, J.; Murray, J. A. *Sci. Transl. Med.* **2013**, *5*, 1−10.

DOI: 10.1021/jacs.6b07483
J. Am. Chem. Soc. 2016, 138, 12278−12286